AD-A280 250

||||||||||||||||||||||||

(barcode)

ARMY RESEARCH LABORATORY

ARL

Thermomechanical Studies of Tungsten Heavy Alloys.

Kenneth F. Ryan and Robert J. Dowding

ARL-TR-447   May 1994

DTIC
S ELECTE
  JUN 1 3 1994
G   D

DTIC QUALITY INSPECTED 2

94-18209

||||||||||||||||||||||||

94 6 13   101

REPORT DOCUMENTATION PAGE

Public reporting burden for this collection of information is estimated to average 1 hour per response, including the time for reviewing instructions, searching existing data sources, gathering and maintaining the data needed, and completing and reviewing the collection of information. Send comments regarding this burden estimate or any other aspect of this collection of information, including suggestions for reducing this burden, to Washington Headquarters Services, Directorate for Information Operations and Reports, 1215 Jefferson Davis Highway, Suite 1204, Arlington, VA 22202-4302, and to the Office of Management and Budget, Paperwork Reduction Project (0704-0188), Washington, DC 20503.

1. AGENCY USE ONLY (Leave blank)	2. REPORT DATE May 1994	3. REPORT TYPE AND DATES COVERED Final Report

4. TITLE AND SUBTITLE

Thermomechanical Studies of Tungsten Heavy Alloys

5. FUNDING NUMBERS

6. AUTHOR(S)

Kenneth F. Ryan and Robert J. Dowding

7. PERFORMING ORGANIZATION NAME(S) AND ADDRESS(ES)

U.S. Army Research Laboratory
Watertown, MA 02172-0001
ATTN: AMSRL-MA-CD

8. PERFORMING ORGANIZATION REPORT NUMBER

ARL-TR-447

9. SPONSORING/MONITORING AGENCY NAME(S) AND ADDRESS(ES)

U.S. Army Research Laboratory
2800 Powder Mill Road
Adelphi, MD 20783-1197

10. SPONSORING/MONITORING AGENCY REPORT NUMBER

11. SUPPLEMENTARY NOTES

12a. DISTRIBUTION/AVAILABILITY STATEMENT

Approved for public release; distribution unlimited.

12b. DISTRIBUTION CODE

13. ABSTRACT (Maximum 200 words)

This report describes the ongoing thermomechanical studies of tungsten heavy alloys at the Materials Directorate of the Army Research Laboratory. Building upon previous work, the data obtained has been correlated to microstructural features before and after testing and evaluated using well known constitutive relations. In past efforts a 91% tungsten heavy alloy was examined. This work examines the effect of strain rate and temperature on a 91% and a 97% heavy alloy and a commercially pure (100%) tungsten. The apparent occurrence of dynamic recrystallization is also discussed.

14. SUBJECT TERMS

Tungsten heavy alloys, Strain rate, Microstructure, Arrhenius equation, Recrystallization, Activation energy

15. NUMBER OF PAGES 20

16. PRICE CODE

17. SECURITY CLASSIFICATION OF REPORT	18. SECURITY CLASSIFICATION OF THIS PAGE	19. SECURITY CLASSIFICATION OF ABSTRACT	20. LIMITATION OF ABSTRACT
Unclassified	Unclassified	Unclassified	UL

Contents

Figures

Table

For

RA&I   ☒
AB   ☐
nced   ☐
ion

tion /

Availability Codes	
Dist	Avail and / or Special
A-1	

iii

INTRODUCTION AND BACKGROUND

A. Deformation

Dynamic thermomechanical testing (TMT) of tungsten heavy alloys (WHA) and commercially pure tungsten is the focus of this work. The dynamic properties were obtained using the Gleeble 1500 over a wide range of temperatures and strain rates. Evaluation of this data depends upon the choice of constitutive equation(s) and the material model of the physical processes occurring. The approach used in the previous work was to mathematically fit the data to a classical strain rate and temperature dependent flow stress equation. This was used to describe the material's flow behavior in terms of either strain, strain rate or temperature. An in-depth discussion of this background can be found in references [1,2]. A power law expression of the form;

$$\sigma = A \, (d\epsilon/dt)^m \qquad (1)$$

describes the dependance between strain rate and stress, at constant temperature and strain. The constant A is the stress at a strain rate of one and m is the strain rate sensitivity and is determined by the slope of a log-log plot of this equation. An additional representation of the flow stress can be made by using the Arrhenius equation;

$$\sigma = C \, \exp(Q/RT) \qquad (2)$$

Where Q is the activation energy of the thermally activated process, R is the universal gas constant, T is the absolute temperature ($^\circ$K) and C is a material dependent constant. The slope at any point of a plot of ln σ versus 1/T is the value of Q/R. This is most informative when this plot results in a straight line and the activation energy can be described over a wide range of temperatures.

This study examined tungsten heavy alloys that are essentially composite materials produced by powder metallurgy techniques. The microstructure of a typical heavy alloy is shown in Figure 1(a). Note that the rounded grains are the tungsten phase. The material surrounding is a multi component matrix phase most often consisting of nickel with iron, cobalt and copper as common additives. The models discussed above do not include the microscopic details of the interactions of the tungsten heavy alloy phases. Nonetheless the description provided by these relationships suggested that some specific types of microscopic deformation occurred.

B. Recrystallization

Recrystallization (static or dynamic) is the process by which strain-free grains grow from mechanically worked grains. The following observations have been made summarizing the effect of time, temperature and deformation on recrystallization kinetics and can be applied to either static or dynamic recrystallization [3-5].

- A minimum deformation (total strain) is required to cause recrystallization
- An inverse relationship exists between total strain and recrystallization temperature, ie. the smaller the degree of deformation, the higher the temperature of recrystallization.
- Increased annealing times result in lower recrystallization temperatures.
- Larger original grain sizes require greater total strains to observe equivalent recrystallization temperatures and times.
- The higher the melting point of the material, the higher the recrystallization temperature.

Dynamic recrystallization is a process that can occur within a metal or alloy while deformation is in progress. That is, when the deformation temperature is sufficiently high, new strain free grains are being formed as the deformation progresses. Previous studies of dynamic recrystallization have generally used the total strain and stress at the onset of recrystallization as the sole parameter of the process [6]. Additional work suggests that, when dynamic recrystallization occurs, the strain at the peak stress is related to the critical strain for the onset of recrystallization. Also, the rate of decrease in flow stress after the peak is related to the rate of recrystallization [7]. It is also known that the temperature dependance of the critical strain influences the recrystallization behavior during hot working. It is also seen that the rate of recrystallization increases with increasing temperature while the time required falls concomitantly. Whether recrystallization occurs during a metalworking process depends on the severity of the operation and the recrystallization temperature as described above. In tungsten heavy alloys, for example, the static recrystallization temperature of the tungsten phase has been observed to be as low as 800°C [5].

As previously described, the tungsten heavy alloys are two component composites consisting of tungsten grains surrounded by a matrix phase. The tungsten grains are essentially pure tungsten. While the matrix phase is an alloy of nickel with iron, cobalt and/or copper with all the tungsten that can be taken into solution. When separately examined the properties of each phase are unique. The tungsten is body centered cubic while the matrix is face centered cubic. Tungsten alone can be quite brittle while the matrix alloy is very ductile. These two components result in a composite that has high density and mechanical properties that are structurally useful. It could also be expected that the two phases would respond to mechanical working and thermal treatments in different ways. For example, aging of the heavy alloy depends on the solubility of the matrix in the tungsten grains [8-10]. It is also known that the matrix and tungsten phases will have different recrystallization temperatures [11]. Under certain circumstances of cold work and annealing the matrix phase may be fully recrystallized while the tungsten phase will remain in the cold worked condition. Which is a strong reminder that the definition of cold working is work that occurs below the recrystallization temperature.

EXPERIMENTAL PROCEDURE

Right circular cylinders of the tungsten-based materials were fabricated with length to diameter ratios of 1.5. For convenience, the specimens were sliced from stock that was already ground to a previously selected diameter for another application. As a result, the diameters of each slightly varied. The ends of the specimens were ground flat and parallel within ± 0.013 mm.

The diameters, along with the nominal chemical composition of the alloys are shown in Table 1. Also shown are the quasistatic mechanical properties of these alloys, as previously determined and reported in reference [12]. The microstructures of the alloys tested are shown in Figure 1 (a,b, and c). The two heavy alloys clearly show the two-phase nature of those materials while the pure tungsten has a highly elongated microstructure that results from the extrusion processing to which that material is typically subjected.

TABLE 1

Composition, Mechanical Properties and Size of Specimens Tested

Alloy	Dia. mm	L/D	Nominal Composition wt%				0.2% Y.S. MPa	UTS MPa	elong
			Ni	Fe	Co	Cu			
91W	6.10	1.5	4.5	2.0	2.5	---	1275	1285	9.4 %
97W	6.22	1.5	1.6	0.7	0.1	0.5	1029	1036	3.1 %
100W	6.35	1.5	---	---	---	---	----	----	---

A full schematic description of the *Gleeble test setup* and associated data acquisition apparatus is shown in references [1,2]. All testing was done in compression in the temperature range 600° to 1200°C. The heating of the specimens was accomplished by electrical self-resistance and controlled by a type K feedback thermocouple percussion welded to the specimen. The strain rates applied were between 2.5 x 10^{-2} and 2.5 x 10^{0} per second and the total true compressive strain was nominally 20%. As done in the previous work [1,2], a 1200°C anneal, for five minutes, was applied to the test specimens *in situ* in the Gleeble apparatus. This was required since the materials were supplied in the worked and aged condition and the strengths exceeded the capacity of the hydraulic ram and the associated load cell. Because of the anneal, the hardness of the specimens was observed to decrease from HRC 37 to less than HRC 20. All testing, including the anneal were done in a vacuum of less than 4 x 10^{-4} torr. Heating and free cooling rates were found consistent from specimen to specimen.

RESULTS AND DISCUSSION

Figure 2 (a, b and c) shows the true stress-true strain results of the 91% heavy alloy at temperatures, 600°, 800°, 1000° and 1200°C at average strain rates of 2.5 x 10^{-2}, 2.5 x 10^{-1} and 2.5 x 10^{0} sec^{-1}. The thermomechanical response of this material was as expected, as it behaved in the classical manner, ie. thermal softening. At all strain rates the yield and flow stresses were observed to decrease with increasing temperature. The work hardening behavior of this alloy was positive at lower temperatures while at the elevated temperatures it was characterized by a neutral

behavior (zero slope). This was seen at all strain rates examined. Similar results can be reported for the 97% heavy alloy except that the work hardening was observed for all conditions except the slowest strain rate at 1000 and 1200° C where flow softening was seen. In the commercially pure material (100W), no flow softening occurred and work hardening was only noticeable at the highest strain rate (2.5×10^0 sec^{-1}). Figure 3 (a and b) shows the results of the 97% and 100% tungsten compression testing performed at the lowest strain rate. In examining the details of the curves in Figures 2a, 3a and possibly in 2b there is a noticeable waviness in the flow curve. This occurs at low strains in 2a and 3a while at higher strains in 2b. In previous work this has suggested dynamic recrystallization in other materials [13]. In working at low strain rates and high temperatures it is typical to expect periodic recrystallization. What is not certain is which phase is undergoing the recrystallization and whether the recrystallization is occurring at other strain rates since it is likely masked by the work hardening. Metallographic evidence will be discussed later in this section.

The flow data was examined in two forms. First the flow stress at 10% strain, for all of the strain rates, was plotted versus the test temperature. This information is grouped by material and is shown in Figure 4 (a,b and c). The slopes, $d\sigma/dT$, of these curves are very similar for the 91W and 97W and are steeper than the curves for the 100W. Calculated values of these slopes, over the temperature range 600-1200°C, are -0.65, -0.63 and -0.27 MPa/°C respectively. The influence of the nickel based matrix is seen quite dramatically in comparing the slopes of the pure tungsten to those of the heavy alloys. The heavy alloy curves are steeper by more than a factor of two. The slope difference is a result of the significant softening of the matrix phase. Recall that the melting point, T_m, of the matrix phase is approximately 1450°C and that most of this study was done at temperatures exceeding $0.5T_m$ where the strength and hardness of that phase can be expected to be quite low. With the two heavy alloys, an observation that can be made is that the slopes appear to increase slightly as the strain rate decreases, suggesting that recrystallization is contributing to the softening and is more dominant at those low strain rates.

The second approach to evaluating the data employed Arrhenius plots of the flow stress at 10% strain. These plots are shown in Figure 5 (a,b and c). There are three strain rates represented on each plot. This is most easily seen for the 100% tungsten. The activation energy for the flow behavior of these materials was determined from the slope of these curves and revealed some unique features of the deformation. The activation energy (Q) for the deformation process was most easily calculated for the pure tungsten. Averaging the three curves gave the result; 9.4 KJ/mole. The situation for the heavy alloys was more difficult as a complex deformation behavior was revealed. The three strain rates can be seen to have very different slopes at high and low temperatures. The consequence is six curves for each of the two heavy alloys, three at the elevated temperatures and three for the lower ones. It appears that an inflection point occurs at approximately 800° C (this point may occur at higher or lower temperatures but the temperature interval used here does not allow for a more accurate definition of this transition). Anyway, the data for the 91W and 97W were combined and the average activation energies were calculated for each of the two temperature regimes. At high temperatures (> 800°C) Q = 6.7 KJ/mole, while at low temperatures (< 800°C) Q = 30.0 KJ/mole. In the heavy alloys, the activation energy at high

4

temperature is nearly identical to the activation energy of the 100W over the entire temperature range. It is believed that the significance of the dual activation energies relates to the alloy phase undergoing deformation in each temperature regime. At low temperatures, the matrix phase is first being work hardened to the strength of the tungsten phase. This work hardening is occurring because the matrix is initially weaker than the tungsten phase. When the two phases become equal in strength, the load is then carried by each phase in proportion to their volumes. At high temperature the matrix phase has no role in the deformation or load carrying and the load must be borne by the tungsten phase alone.

There are several microstructural features of interest in the specimens tested that allow for some of the conclusions above. For comparison, the reader's attention is directed to Figure 1 (a,b and c), the microstructures of the pretest material. Figure 6 (a,b,c and d) contains the post test microstructure of four 97W specimens corresponding to the four temperatures of interest. These specimens were subjected to the slowest strain rate used. The most salient feature in these micrographs is the clear progression of tungsten to tungsten grain contact failure and decohesion of the tungsten/matrix interface as the test temperature increases. It is the most pronounced at 1200° C. A less obvious feature is seen within the tungsten grains themselves. The microstructure of the heavy alloy at the lower temperatures shows uniform deformation of the tungsten and matrix phases after the 20% total applied strain. At the higher temperatures, the deformation is entirely concentrated within the tungsten grains and is manifested by the presence of slip bands within the grains. It is interesting to note that the slip deformation in the tungsten grains in the heavy alloys does not appear in all of the grains. The likely cause is the single crystal nature of these grains and that they are in random orientations to the deformation. Some of the crystallographic directions and planes of these grains are oriented to the plane of observation in such a way that the deformation is apparent in the micrograph. Similar results were observed for the 91W material and one example is shown in Figure 7. The 100W material, because it was single phase and had a highly elongated microstructure, did not suffer from decohesion as seen in the heavy alloys but exhibited slip at all temperatures. This is shown in Figure 8. In a manner similar to the heavy alloys slip is not seen in all of the grains, only in the grains favorably oriented to the plane of view.

SUMMARY

Thermomechanical testing of two tungsten heavy alloys and a commercially pure tungsten in the temperature range 600 to 1200° C at strain rates up to 2.5 sec^{-1} gave the following results.

All materials thermally softened in classic response to increasing test temperature. The rate of softening with increasing temperature (dσ/dT) was calculated and found to be more than twice as great for the heavy alloys in comparison to the pure tungsten. This response was attributed to the increased rate of strength loss in the matrix phase.

Through Arrhenius plots; the heavy alloys were found to change their deformation behavior as the temperature increased over 800° C. The matrix phase again was identified as the reason for

5

the variation. It was concluded that the tungsten phase is responsible for carrying the load at elevated temperatures.

Examination of the metallographic data revealed that as the temperature increased a greater number the tungsten grain contacts failed. It was also seen that the tungsten/matrix interface increasingly failed. Of particular note was that at the highest temperatures, the tungsten phase showed deformation slip bands that had not been seen in the lower temperature regime. This suggested that at below 800° C the deformation was uniform but at high temperature it is concentrated in the tungsten grains.

REFERENCES

1. K.F. Ryan and R.J. Dowding, International Conference on Tungsten and Tungsten Alloys-1992, MPIF, Princeton, NJ, 1993, pp 249-56.
2. K.F. Ryan and R.J. Dowding, "Yield Properties of Tungsten and Tungsten Heavy Alloys", Army Research Laboratory, ARL-TR-143, June 1993.
3. G.E. Dieter, Mechanical Metallurgy, McGraw-Hill Book Company, New York, 1979.
4. R.E. Reed-Hill, Physical Metallurgy Principles, Litton Educational Publishing, Inc., Monterey, CA, 1973.
5. R.J. Dowding, "The Recrystallization and Respheriodization of Tungsten Grains in a Tungsten Heavy Alloy", Recrystallization '90, TMS, Warrendale, PA, 1990.
6. Wray, Met. Trans. A, vol. 15A, no. 11, 1984, p 2009.
7. Glover and Sellars, Met. Trans. A, vol. 4A, no. 3, 1973, p 767.
8. J.B. Posthill and D.V. Edmonds, Mater. Res. Soc. Symp. Proc., 21, 811, 1984.
9. J.B. Posthill, Proc. 42nd Ann. Meet. Electron Microscopy Society of America, Ed. G.W. Bailey, 488 (1984).
10. J.B. Posthill, R.J. Dowding and K.J. Tauer, International Conference on Tungsten and Tungsten Alloys-1992, MPIF, Princeton, NJ, 1993, pp 437-44.
11. M. Yodogawa, Sintering-Theory and Practice, D. Kolar, S. Pejovnik and M.M. Restic, eds., Elsevier Publishing Co., 1982.
12. P. Woolsey, R.J. Dowding, K.J. Tauer and F.S. Hodi, International Conference on Tungsten and Tungsten Alloys-1992, MPIF, Princeton, NJ, 1993, pp 533-40.
13. J.J. Jonas and T. Sakai, 1982 ASM Materials Science Seminar on Deformation, Processing and Structure, G. Krauss, ed., ASM, Materials Park, Ohio, 1982, pp 185-228.
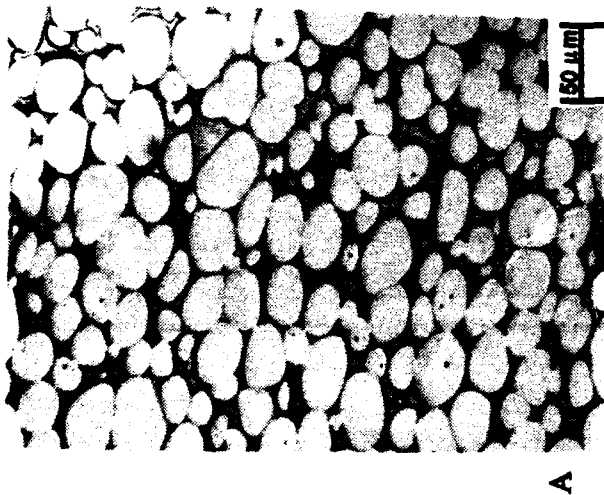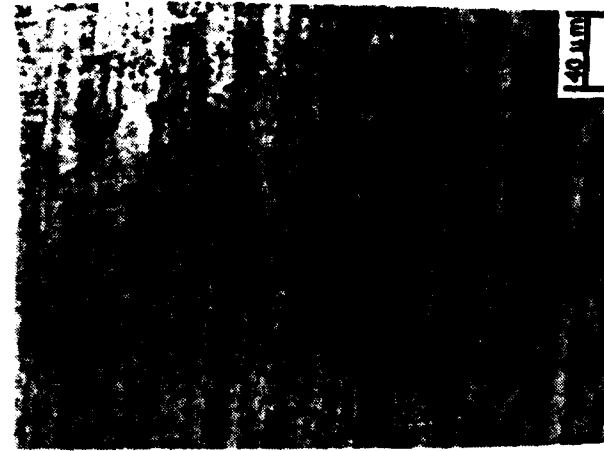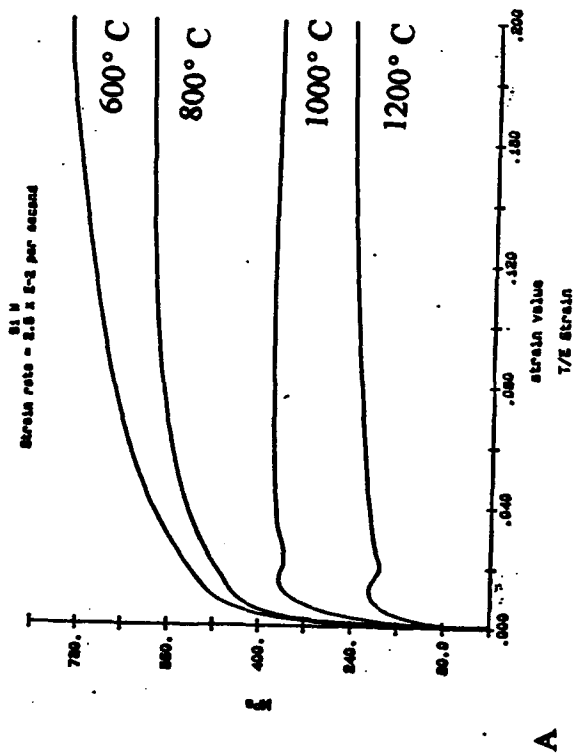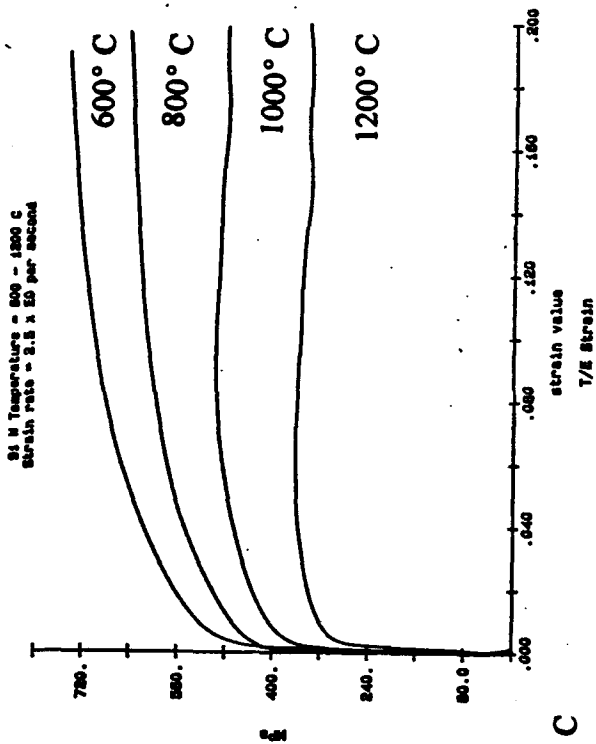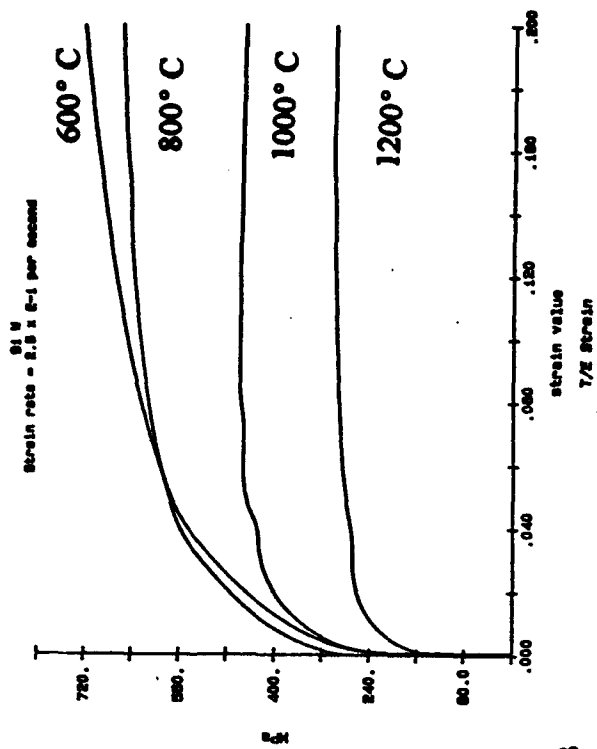
Figure 1. Pre test microstructural features; (A) 91% tungsten heavy alloy, (B) 97% tungsten heavy alloy and (C) commercially pure tungsten. Note the rounded grains of the heavy alloys and the nickel rich matricies that bond the grains. The pure tungsten is heavily drawn.

Figure 2. Compressive true stress-true strain results for the 91% tungsten heavy alloy at three strain rates; (A) 2.5×10^{-2} sec^{-1}, (B) 2.5×10^{-1} sec^{-1}, and (C) 2.5×10^{0} sec^{-1}.
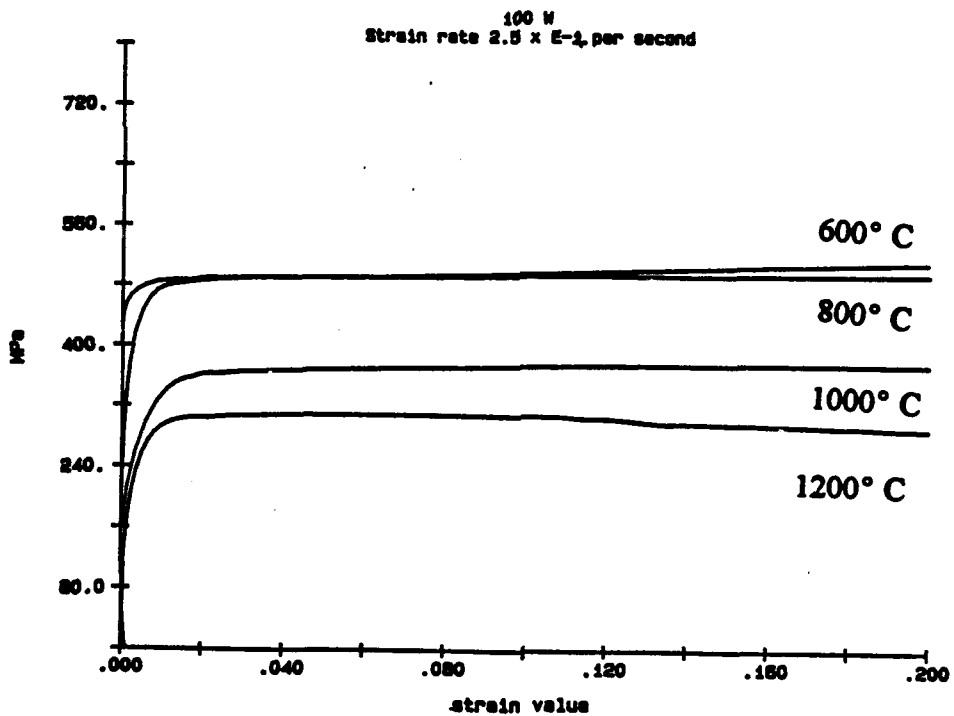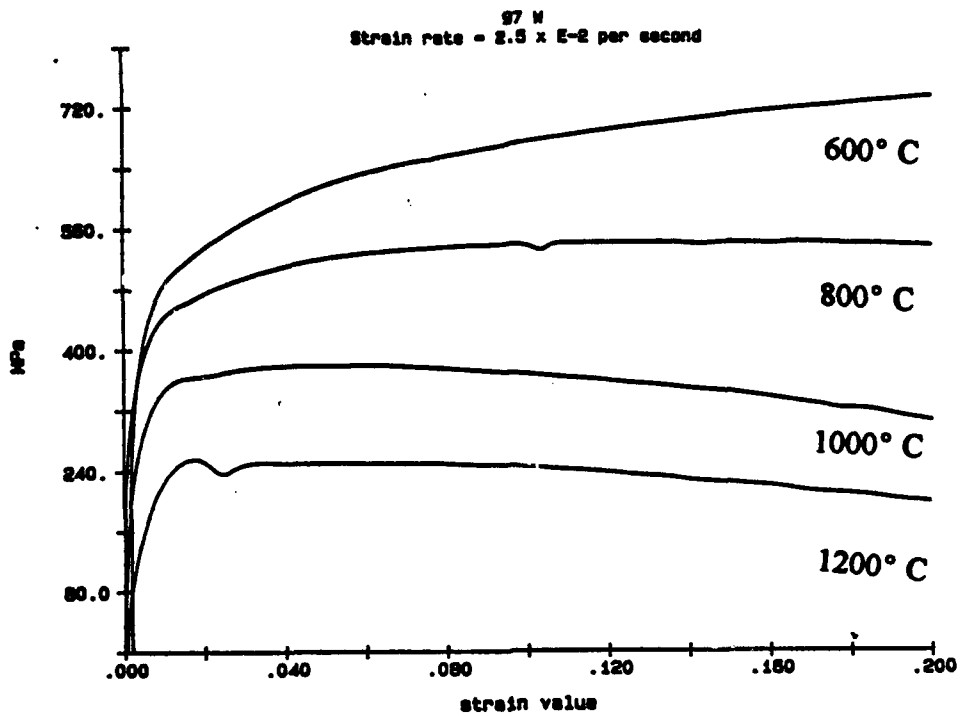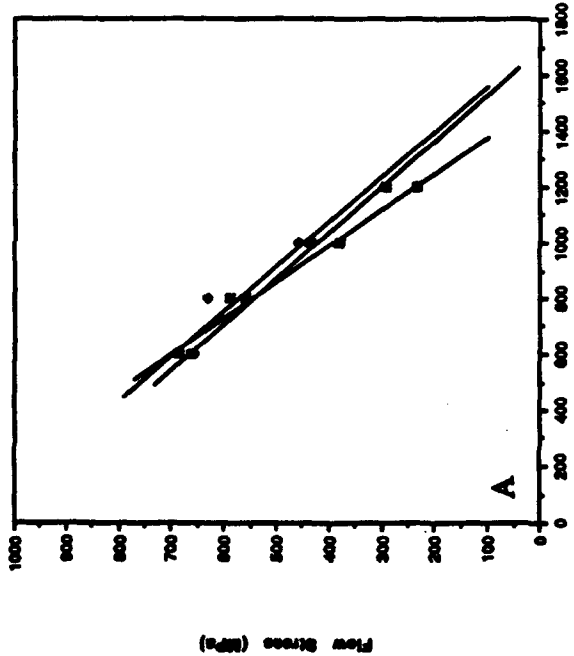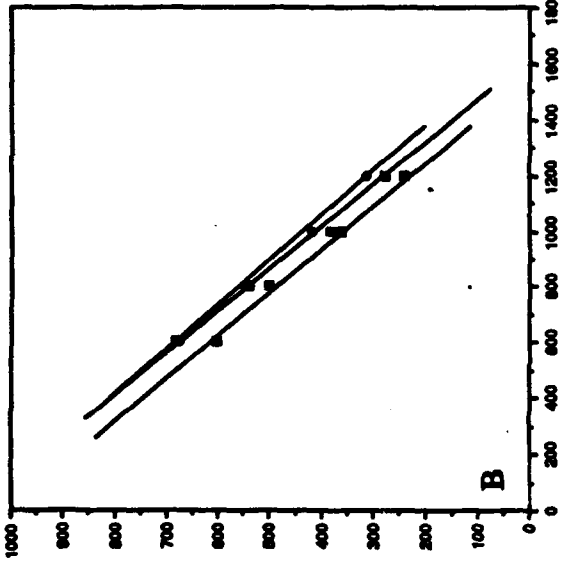
A

B

Figure 3, Compressive true stress-true strain results for (A) 97% heavy alloy and (B) commercially pure tungsten. Both tests at a strain rate of 2.5 x 10^{-2} sec^{-1}. Compare to Figure 2A.

Flow Stress vs. Temperature for 100W

Flow Stress vs. Temperature for 97W

Flow Stress vs. Temperature for 91W

Temperature (°C)

Temperature (°C)

Temperature (°C)

Flow Stress (MPa)

Strain Rates / Second

■ 2.5 x 10e-2

◆ 2.5 x 10e-1

■ 2.5 x 10e0

A

B
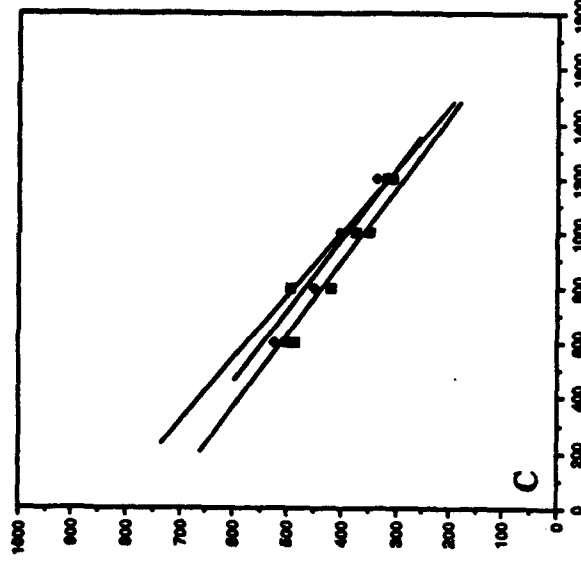
C

Figure 4, Flow stress at 10% strain versus the test temperature at all of the strain rates used; (A) 91% heavy alloy, (B) 97% heavy alloy and (C) 100% tungsten.

10
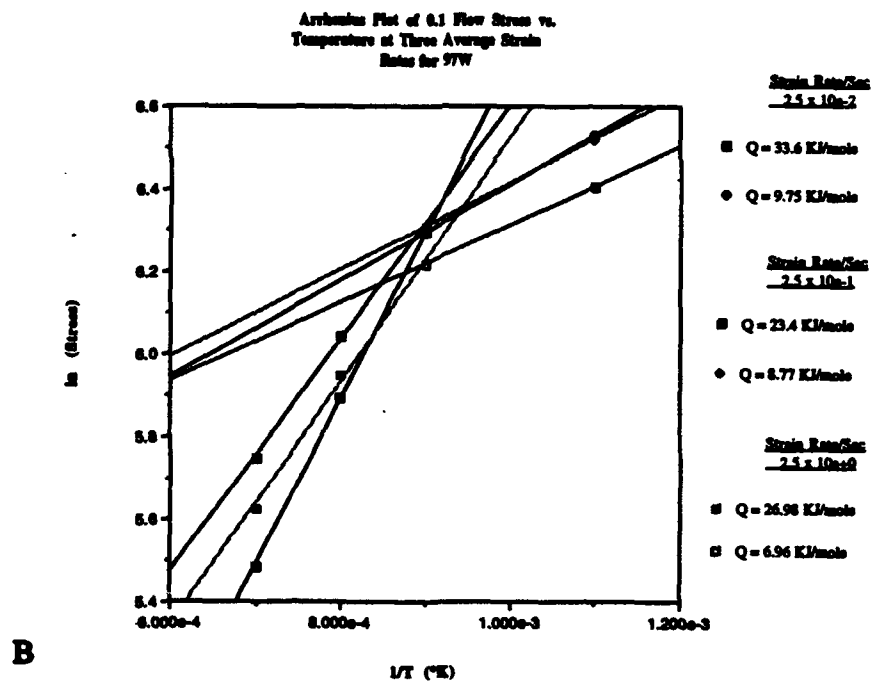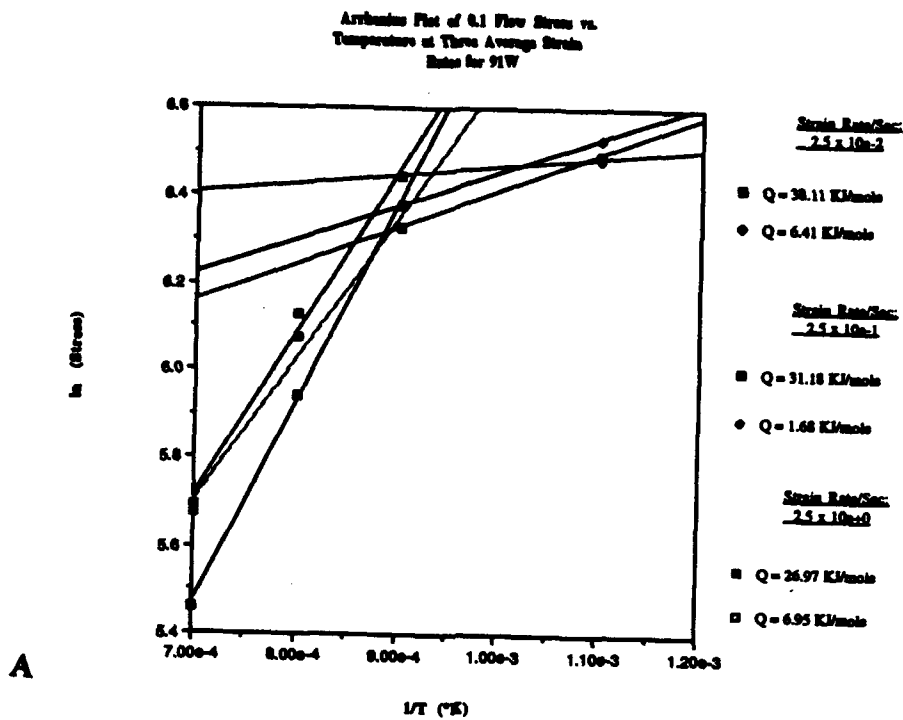
Figure 5. Arrhenius plots of the 10% strain flow stress versus the reciprocal temperature for each of the strain rates used; (A) 91% heavy alloy, (B) 97% heavy alloy and (C) 100% tungsten.

Arrhenius Plot of 0.1 Flow Stress vs.
Temperature at Three Average Strain
Rates for 100 W

STRAIN RATE/SEC

■ 2.5 x 10e-2

● 2.5 x 10e-1

■ 2.5 x 10e0

ACTIVATION ENERGY

Q = 10.03 KJ/mole

Q = 8.96 KJ/mole

Q = 9.16 KJ/mole

Figure 5. C

12
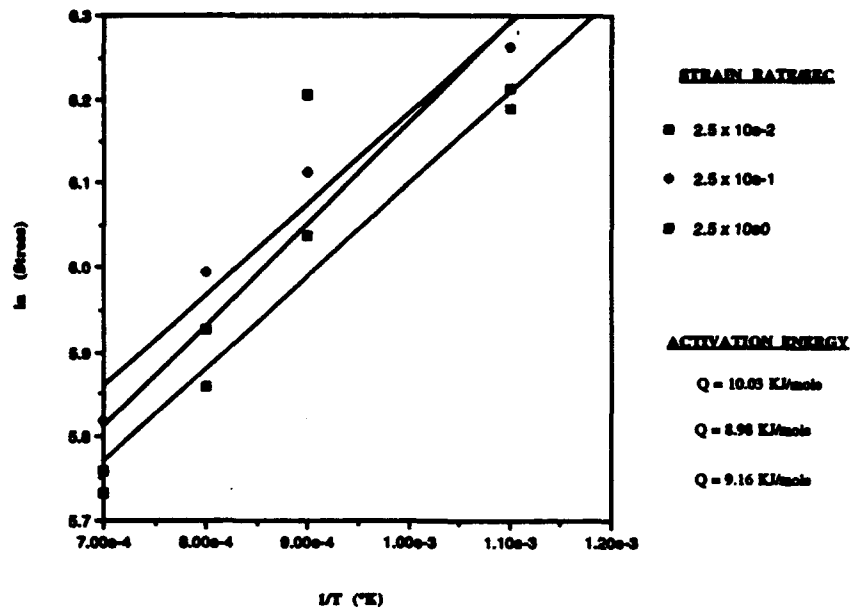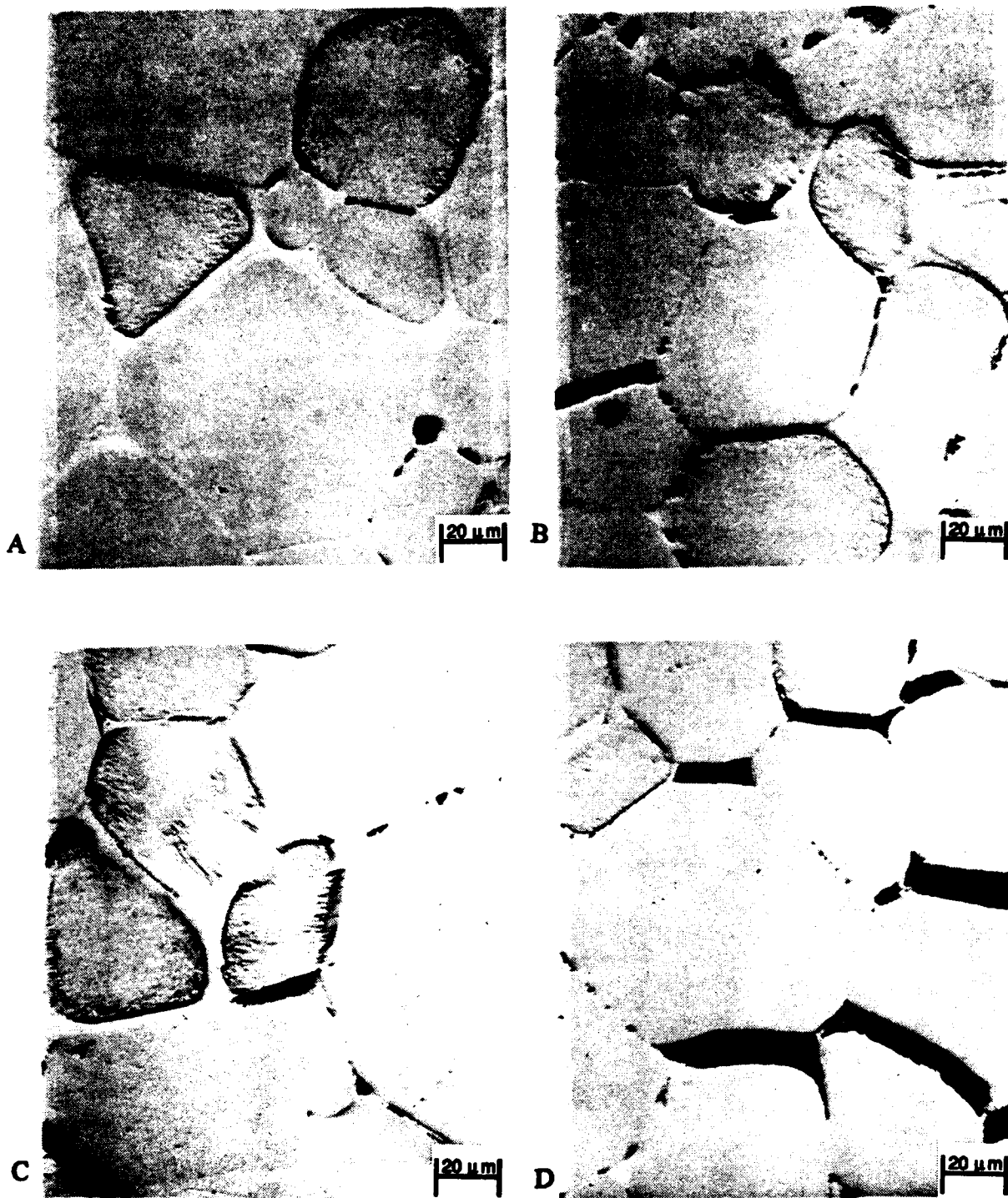
Figure 6. Post test microstructural features of the 97% tungsten heavy alloy. Strain rate 2.5×10^{-2} sec^{-1}. Test temperatures; (A) 600, (B) 800, (C) 1000 and (D) 1200° C.

Figure 7. Post test microstructural features of the 91% tungsten heavy alloy tested at a strain rate of 2.5×10^{-1} sec^{-1} and a temperature of 1000° C.

Figure 8. Post test microstructure of a 100% tungsten specimen tested at 2.5×10^{-2} sec^{-1} at a temperature of 1200° C.
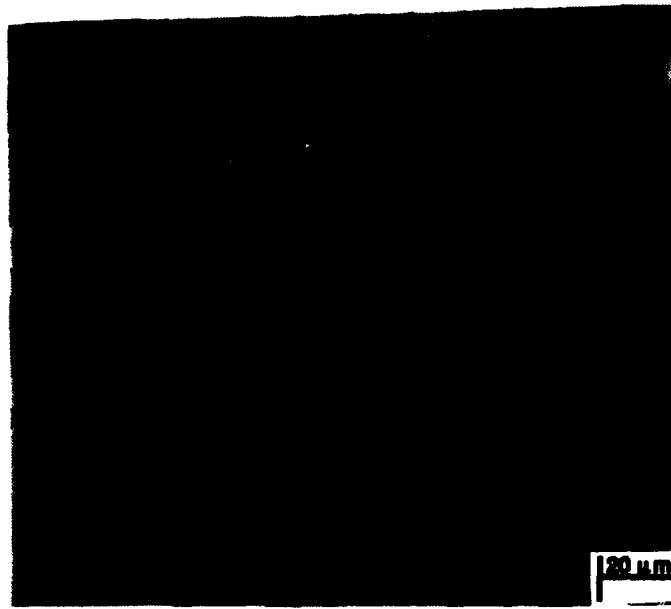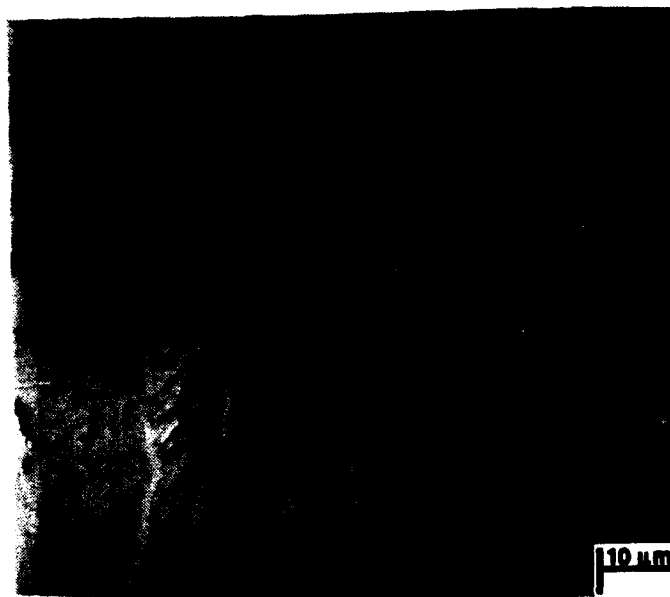
DISTRIBUTION LIST

No. of Copies	To
1	Office of the Under Secretary of Defense for Research and Engineering, The Pentagon, Washington, DC 20301

Director, U.S. Army Research Laboratory, 2800 Powder Mill Road, Adelphi, MD 20783-1197

No. of Copies	To
1	ATTN: AMSRL-OP-SD-TP, Technical Publishing Branch
1	Dr. Alan Goldman
1	AMSRL-OP-SD-TM, Records Management Administrator

Commander, Defense Technical Information Center, Cameron Station, Building 5, 5010 Duke Street, Alexandria, VA 23304-6145

2	ATTN: DTIC-FDAC
1	MIA/CINDAS, Purdue University, 2595 Yeager Road, West Lafayette, IN 47905

Commander, Army Research Office, P.O. Box 12211, Research Triangle Park, NC 27709-2211

1	ATTN: Information Processing Office
1	Dr. Andrew Crowson
1	Dr. Edward Chen

Commander, U.S. Army Materiel Command, 5001 Eisenhower Avenue, Alexandria, VA 22333

1	ATTN: AMCSCI

Commander, U.S. Army Materiel Systems Analysis Activity, Aberdeen Proving Ground, MD 21005

1	ATTN: AMXSY-MP, H. Cohen

Commander, U.S. Army Missile Command, Redstone Arsenal, AL 35809

1	ATTN: AMSMI-RD-CS-R/Doc

Commander, U.S. Army Armament, Munitions and Chemical Command, Dover, NJ 07801

1	ATTN: Technical Library
1	Mr. D. Kapoor
1	Dr. S. Cytron
1	Mr. K. Wilson

Commander, U.S. Army Tank-Automotive Command, Warren, MI 48397-5000

2	ATTN: AMSTA-TSL, Technical Library

Commander, U.S. Army Foreign Science and Technology Center, 220 7th Street, N.E., Charlottesville, VA 22901-5396

3	ATTN: AIFRTC, Applied Technologies Branch, Gerald Schlesinger

Naval Research Laboratory, Washington, DC 20375

1	ATTN: Code 2627
1	Dr. Virgil Provenzano

Chief of Naval Research, Arlington, VA 22217

1	ATTN: Code 471

No. of Copies	To

Naval Surface Weapons Center, Dahlgren, VA 22448
1   ATTN: Code G-32, Ammunition Branch, Mr. Peter Adams

Commander, Rock Island Arsenal, Rock Island, IL 61299-6000
1   ATTN: SMCRI-SEM-T

Battelle Columbus Laboratories, Battelle Memorial Institute, 505 King Avenue, Columbus, OH 43201
1   ATTN: Mr. Henry Cialone
1   Dr. Alan Clauer

Battelle Pacific Northwest Laboratories, P.O. Box 999, Richland, WA 99352
1   ATTN: Mr. William Gurwell
1   Dr. Gordon Dudder
1   Mr. Curt Lavender

GTE Sylvania, Inc. Chemical Metallurgical Division, Hawes Street, Towanda, PA 18848
1   ATTN: Dr. James Mullendore
1   Mr. James Spencer
1   Ms. Susan Doepker

Director, U.S. Army Research Laboratory, Aberdeen Proving Ground, MD 21005
1   ATTN: AMSRL-WT
1   AMSRL-WT-T, Dr. Lee Magness
1   Ms. W. A. Leonard

Teledyne Advanced Materials, 1 Teledyne Place, La Vergne, TX 37086
1   ATTN: Dr. Steven Caldwell

Los Alamos National Laboratory, ATAC, MS F681, P.O. Box 1663, Los Alamos, NM 87545
1   ATTN: Mr. Bill Hogan
1   Mr. Paul Dunn
1   Mr. Bill Baker

Philips Elmet, 1560 Lisbon Road, Lewiston, ME 04240
1   ATTN: Mr. James Anderson

Ultramet, Inc., 12173 Montague Street, Pacoima, CA 91331
1   ATTN: Mr. Brian Williams
1   Dr. Robert Tuffias

Ceracon, Inc., 1101 N. Market Boulevard, Suite 9, Sacramento, CA 95834
1   ATTN: Dr. Ramas Raman
1   Mr. Sundeep Rele

Southwest Research Institute, 6220 Culebra Road, P.O. Drawer 28510, San Antonio, TX 78228-0510
1   ATTN: Dr. James Lankford
1   Dr. Herve Couque
1   Dr. Charles Anderson

No. of Copies	To
	Metalworking Technology, Inc., 1450 Scalp Avenue, Johnstown, PA 15904
1	ATTN: Mr. C. Buck Skena
1	Mr. Timothy McCabe
	Research Triangle Institute, P.O. Box 12194, Research Triangle Park, NC 27709-2154
1	ATTN: Dr. John B. Posthill
	3C Systems, 620 Arglye Road, Wynnewood, PA 19096
1	ATTN: Mr. Murray Kornhauser
	Advance Technology Coatings, 300 Blue Smoke Court, West, Fort Worth, TX 76105
1	ATTN: Dean Baker
	Alliant Techsystems, 7225 Northland Drive, Brooklyn Park, MN 55428
1	ATTN: Dr. Stan Nelson
1	Mr. Mark Jones
	SPARTA, Inc., CAMDEC Division, 2900-A Saturn Street, Brea, CA 92621-6203
1	ATTN: John A. Brinkman
	Chamberlain Manufacturing Co., 550 Esther St., P.O. Box 2545, Waterloo, IA 50704
1	ATTN: Mr. Tom Lynch
	Defense Technology International, Inc., The Stark House, 22 Concord Street, Nashua, NH 03060
1	ATTN: Mr. Douglas Ayer
	Materials and Electrochemical Research Corporation, 7960 S. Kolb Road, Tucson, AZ 85706
1	ATTN: Dr. James Withers
1	Dr. Sumit Guha
	Materials Modification, Inc., 2929-P1 Eskridge Center, Fairfax, VA 22031
1	ATTN: Dr. T. S. Sudarshan
	Micro Materials Technology, 120-D Research Drive, Milford, CT 06460
1	ATTN: Dr. Richard Cheney
	Nuclear Metals, 2229 Main Street, Concord, MA 01742
1	ATTN: Dr. William Nachtrab
	Olin Ordnance, 10101 9th Street N., St. Petersburg, FL
1	ATTN: Hugh McElroy
	The Pennsylvania State University, Department of Engineering Science and Mechanics, 227 Hammond Building, University Park, PA 16802-1401
1	ATTN: Dr. Randall M. German, Professor, Brush Chair in Materials
	Worcester Polytechnic Institute, 100 Institute Road, Worcester, MA 01690
1	ATTN: Dr. Ronald Biederman
1	Dr. Richard Sisson

No. of Copies	To

Failure Analysis Associates, Inc., 149 Commonwealth Drive, P.O. Box 3015, Menlo Park, CA 94025

1	ATTN: S. P. Andrew
1	R. D. Caliguri
1	T. K. Parnell
1	L. E. Eiselstein

Amorphous Technologies International, Laguna Hills, CA 92653

1	ATTN: Mr. Dick Harlow

Parmatech Corporation, 2221 Pine View Way, Petaluma, CA 94952

1	ATTN: Dr. Animesh Bose

Stiglich Associates, P.O. Box 206, Sierra Madre, CA 91025

1	ATTN: Dr. Jack Stiglich

Director, U.S. Army Research Laboratory, Watertown, MA 02172-0001

2	ATTN: AMSRL-OP-WT-IS, Technical Library
10	AMSRL-MA-CD, Authors